Progress In Electromagnetics Research Letters, Vol. 65, 123–130, 2017

UWB Heart-Shaped Planar Monopole Antenna with a Reconfigurable Notched Band

Changzhou Hua*, Yunlong Lu, and Taijun Liu

Abstract—This paper presents a heart-shaped planar monopole antenna for ultra-wideband (UWB) applications. To increase the impedance bandwidth of the antenna and achieve UWB coverage, we use a heart-shaped radiating patch fed by a microstrip line and an elliptical curved ground plane. Based on this structure, by etching an annular slot loaded with a capacitor in the heart-shaped radiating patch, a planar band-notched UWB antenna can also be obtained. Specifically, to demonstrate the potential application of the proposed structure, a UWB antenna design with a reconfigurable notched band is presented by using a varactor to replace the capacitor. Commercial software ANSYS HFSS is used to analyze and design this antenna. Measured results of the fabricated antenna show good agreement with simulated ones.

1. INTRODUCTION

The design of ultra-wideband (UWB) antenna has attracted increasing interest since Federal Communication Commission (FCC) assigned the unlicensed use of the 3.1–10.6 GHz band for commercial communication applications [1]. A lot of broadband monopole configurations have been used for this band, but the radiators are perpendicular to the ground planes. Planar monopole antennas have been found to be excellent candidates to operate in UWB wireless systems, since they can be integrated with other components on the same printed circuit board (PCB) and present simple structure, easy fabrication, wideband characteristics, and omnidirectional radiation patterns. Consequently, a number of planar monopole antennas with different geometries have been experimentally characterized [2–6]. In practice, the ultra-wide bandwidth of the UWB systems will cause interference with other narrow band systems such as the WLAN bands (5.15–5.35 GHz and 5.725–5.825 GHz). To reject these interferences, without increasing the system's size and complexity, a simple and effective way is to use UWB antennas with band-notched properties. For the past few years, various approaches have been investigated to design band-notched UWB antennas [7–13]. Generally speaking, there are two distinctive techniques used for achieving band-notched properties of planar antennas. One general technique is to etch various shaped slots in the radiating patch or ground plane [7–10]. Another technique is to load parasitic resonators in or near the feed line [11, 12]. However, these designs have a disadvantage that the notch frequency cannot be easily adjusted after fabrication. Recently, slot resonators loaded with MEMS switches, PIN diodes, or varactor diodes have been used to achieve UWB antennas with an adjustable notched band [14–16].

In this paper, a UWB heart-shaped planar monopole antenna is presented. The antenna consists of a heart-shaped radiating patch fed by a microstrip line and an elliptical curved ground plane [17]. Commercial software ANSYS HFSS is used to analyze and design this antenna. The optimized antenna prototype is designed, fabricated and measured. Meanwhile, by etching an annular slot loaded with a capacitor in the heart-shaped radiating patch, a band-notched UWB antenna prototype can be achieved.

Received 2 December 2016, Accepted 9 January 2017, Scheduled 26 January 2017

* Corresponding author: Changzhou Hua (huachangzhou@nbu.edu.cn).

The authors are with the Faculty of Electrical Engineering and Computer Science, Ningbo University, Ningbo 315211, China.

Based on this prototype, by using a varactor to replace the capacitor, a UWB antenna design with a reconfigurable notched band is finally obtained.

2. ANTENNA DESIGN

2.1. Antenna Structure

The geometry of the proposed UWB planar monopole antenna is shown in Fig. 1. The antenna is printed on a 0.508-mm-thick Rogers Duroid 5880 substrate with a relative permittivity of 2.2 and a loss tangent of 0.0009. It is seen that the planar antenna consists of a heart-shaped radiating patch fed by a microstrip line on the top side of the substrate. Meanwhile, in order to improve the impedance bandwidth, an elliptical curved ground plane is printed on the bottom side of the substrate. The contour of the heart-shaped patch can be expressed as

$$\begin{cases} x = a\,[2\cos(t) - \cos(2t)] \\ y = a\,[2\sin(t) - \sin(2t)] \end{cases} \tag{1}$$

where parameter t varies from 0 to 2π, and parameter a is used to control the size of the heart-shaped patch, which determines the center frequency of the antenna. The length and width of the dielectric substrate are $L = 42\,\text{mm}$ and $W = 30\,\text{mm}$, respectively. Other dimensions of the fabricated UWB monopole antenna are as follows: $W_p = 22.7\,\text{mm}$, $W_f = 1.82\,\text{mm}$, $g = 1.85\,\text{mm}$, $L_p = 18.9\,\text{mm}$, $L_f = 16.8\,\text{mm}$, and $L_g = 13.5\,\text{mm}$.

Commercial software ANSYS HFSS is used to analyze and design this antenna. To validate the simulation results, a prototype of the proposed antenna has been fabricated and measured. Fig. 2 depicts photographs of the top and bottom sides of the prototype. The simulated and measured VSWR results of this antenna are given in Fig. 3. It can be observed that a very good agreement between measured and simulated results is obtained, with the discrepancy caused probably by the fabrication errors. The measured impedance bandwidth is 4.25 : 1 (2.8–11.9 GHz), which covers the entire UWB band. It should be pointed out that, at low frequencies, the input impedance of the antenna is primarily a function of the patch dimensions and essentially independent of the substrate. At high frequencies, the input impedance is strongly affected by the substrate parameters and the spacing between the bottom of the patch and the ground plane. Making the upper edge of the ground plane elliptic can improve the impedance matching [18]. The simulated VSWR results for the antenna with an elliptical curved ground plane and a flat ground plane are also compared in Fig. 3. It can be found that, by using an elliptical curved ground plane, the impedance matching is obviously improved at the high frequencies, which broadens the bandwidth of the antenna.

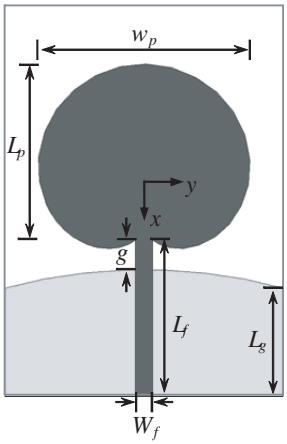

Figure 1. Geometry of the proposed heart-shaped UWB antenna (dark gray: top side, light gray: bottom side).

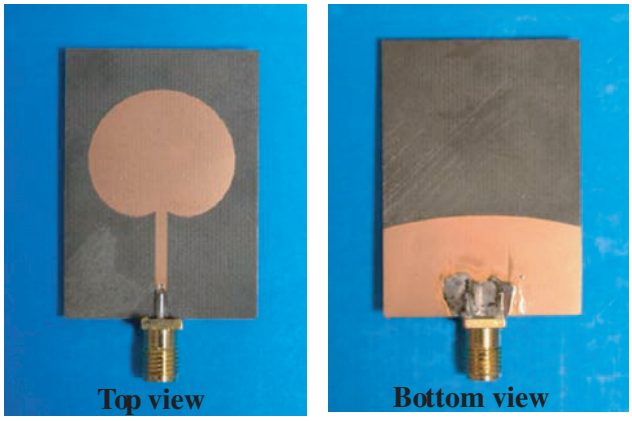

Figure 2. Photographs of the fabricated heart-shaped UWB antenna.

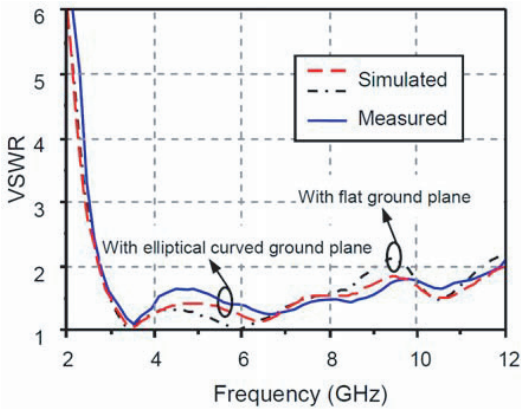

Figure 3. Measured and simulated VSWR results of the heart-shaped UWB antenna.

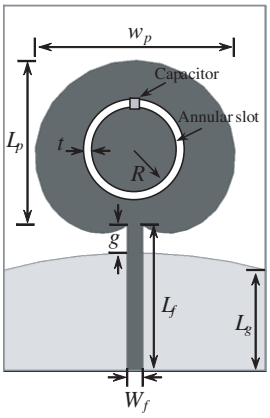

Figure 4. Geometry of the proposed band-notched UWB antenna (dark gray: top side, light gray: bottom side).

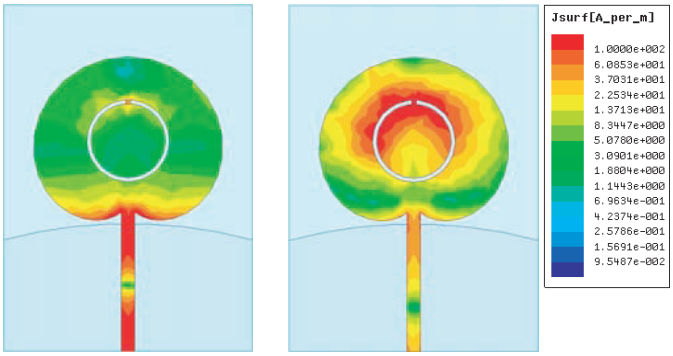

(a) (b)

Figure 5. Surface current distributions of the proposed band-notched UWB antenna at (a) 6 GHz (pass-band frequency), (b) 5 GHz (notched-band frequency).

2.2. Band-Notched UWB Antenna

A band-notched UWB antenna can be achieved by a simple modification of the above design. Fig. 4 shows the geometry of the proposed UWB antenna with a notched band. As shown, an annular slot loaded with a capacitor is etched in the heart-shaped radiating patch, which can be viewed as a split-ring resonator. The critical parameters that impact on the band-notched performance are the width and radius of the slot, and the capacitance of the capacitor. In this design, the width and radius of the slot are $t = 0.5$ mm and $R = 4.5$ mm, respectively. The capacitance of the capacitor is chosen to be 1.5 pF.

The simulated surface current distribution of the antennas is also given to clarify the operation of the band-notched structure on the performance of the UWB antenna. Fig. 5 illustrates the surface currents distribution at the radiating frequency 6 GHz and the notched frequency 5 GHz, respectively. It is seen that the surface currents at 6 GHz mainly distribute along the lower edge of the heart-shaped patch as well as the feed line, which is a major cause of the effective radiation. Simultaneously, very little currents are observed around the capacitor-loaded annular slot. The surface currents at 5 GHz, attributed to the resonance, are clustered around the edge of the annular slot, which results in a low radiation efficiency. The simulated and measured VSWR results of the band-notched UWB antenna are given in Fig. 6, which indicated that by etching an annular slot loaded with a capacitor in the radiating patch, a narrow notched band is created. As shown, the proposed antenna has an impedance bandwidth of 2.8–11.9 GHz for a VSWR less than 2, except the notched frequency band of 4.4–5.4 GHz.

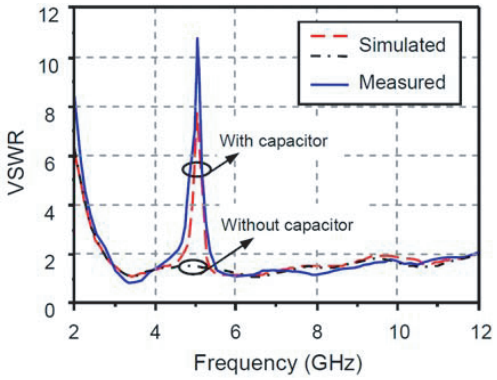

Figure 6. Measured and simulated VSWRs of the band-notched antenna.

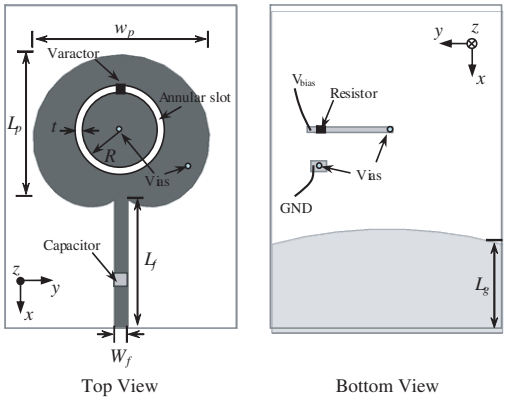

Figure 7. Geometry of the proposed UWB antenna with a reconfigurable notched band.

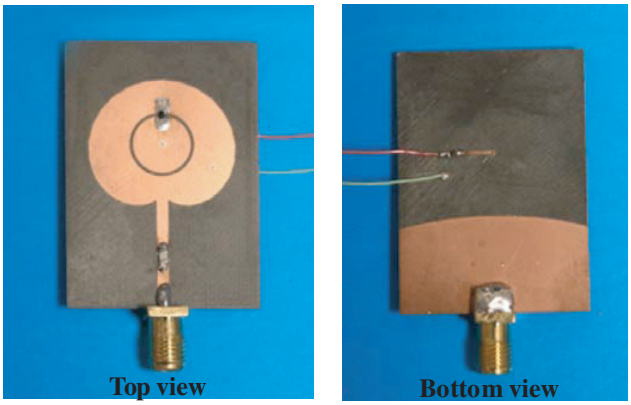

Figure 8. Photographs of the fabricated reconfigurable band-notched UWB antenna.

For comparison, the simulated VSWR for the antenna with the annular slot in the radiating patch but without capacitor loading is also given in Fig. 6. It is seen that the notched band does not appear in this case.

It is also worth noting that if we change the resonant frequency of the annular slot, the location of the notched band will be changed automatically as well. Fortunately, the resonant frequency of the annular slot can be simply tuned by adjusting the capacitance of the capacitor, which means we can control the notched band by using a tunable capacitor. This will be described in detail in the following section.

2.3. Reconfigurable Band-Notched UWB Antenna

Generally speaking, a varactor can be modeled as a tunable capacitor. So by loading a varactor instead of the capacitor (see Fig. 4) on the annular slot, it is expected that reconfigurable notched band will be generated. The geometry of the proposed reconfigurable band-notched UWB antenna is shown in Fig. 7. The annular slot is loaded with a Skyworks SMV1405 varactor [19], which offers a variable capacitance range extending from 0.63 to 2.67 pF for the corresponding tuning reverse bias variation from 30 to 0 V. As shown in Fig. 7, the varactor is across the annular slot on the top side of the substrate. The bias circuit is printed on the bottom side of the substrate, which bias the varactor through vias. Since the varactor's bias current amounts to only a few nano-ampere, a 1-M Ω resistor is used to block RF signals while providing an adjustable reverse bias to the varactor [20]. A DC-blocking capacitor is inserted in the middle of the feeding line to prevent DC current flow through. It should be pointed out that, at pass-band frequency, because the currents distribute around the DC biasing feeding structure is very

weak (see Fig. 5), the influence of the DC biasing feeding structure placed on the bottom layer of the antenna on its radiation characteristics can almost be ignored.

Figure 8 shows photographs of the fabricated reconfigurable band-notched UWB antenna. The measured VSWR results are presented in Fig. 9. The bias voltages applied to the varactor were varied from 30 to 0 V. As shown, the measured VSWRs of the antenna for different values of the DC bias voltage are depicted. It is seen that, the reconfigurable band-notched UWB antenna can cover a notch tuning range extending from 4.62 to 5.83 GHz, which is sufficient to reject the interference with either the lower WLAN (5.15–5.35 GHz) or higher WLAN (5.725–5.825 GHz) services, without affecting the response of the antenna at other frequencies. It's worth mentioning that the band-notching characteristic of this design can be explained by an equivalent parallel RLC circuit, where R, L, and C represent the resistance, inductance, and capacitance of the circuit, respectively [21, 22]. For a parallel RLC circuit, the resonant frequency and the quality factor Q are proportional to $1/\sqrt{LC}$ and $\sqrt{C/L}$, respectively [22]. In our design, the rejection level (VSWR level) of the notched band mainly depends on the quality factor Q, larger Q value leads to deeper rejection. As the DC bias voltage increases, the capacitance of the varactor decreases, which decreases the total capacitance C of the equivalent parallel RLC circuit. Consequently, $1/\sqrt{LC}$ globally increases, while $\sqrt{C/L}$ decreases. As a result, the resonant notched frequency increases, but the Q value decreases, leading to a lower rejection level (VSWR level).

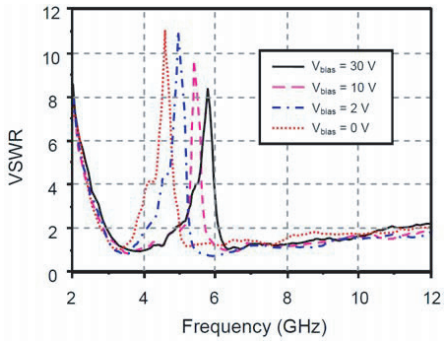

Figure 9. Measured VSWRs of the reconfigurable band-notched antenna for different values of the DC bias voltage from $V_{bias} = 30$ to 0 V.

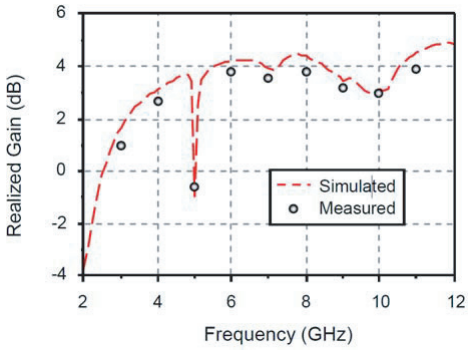

Figure 10. Measured and simulated realized gains of the reconfigurable band-notched antenna ($V_{bias} = 2$ V, $f_{notch\ frequency} = 5.1$ GHz).

2.4. Radiation Characteristics

To investigate the radiation characteristics of the reconfigurable band-notched UWB antenna, the simulated and measured gain results of the antenna are shown in Fig. 10. For the sake of brevity, results are shown only for the case with the varactors' bias tuned to be 2 V. As shown, the measured gains show good agreement with the simulated ones and the proposed antenna exhibits relatively stable gains across the operating bands, except the frequency notched band (around 5.1 GHz), in which the gain values decrease significantly. The small differences between the simulated and experimental results were deemed very acceptable. They arose from the presence of the long feed lines in the measurement setup, and the usual unavoidable errors in the fabrication, installation, and measurement processes.

Figure 11 shows the simulated and measured normalized co- and cross-polarized far-field radiation patterns of the proposed reconfigurable band-notched UWB antenna at 4, 7, and 10 GHz, respectively. As shown, in each case, the figure on the left shows the radiation pattern in the E plane (x-z plane), whereas the H-plane (y-z plane) radiation pattern is depicted on the right. It can be seen that, at low frequency (4 GHz), the proposed antenna has a reasonably omnidirectional pattern in the H plane, whereas the E-plane radiation pattern is similar to the shape of a Fig. 8 (like a dipole). It can also be seen that the radiation pattern deteriorates at the higher frequency (10 GHz), which means that the radiation pattern bandwidth is significantly smaller than the impedance bandwidth. However, if the antenna is to operate in a multi-path environment, the rather erratic radiation patterns at the higher frequencies should not be a limiting factor.

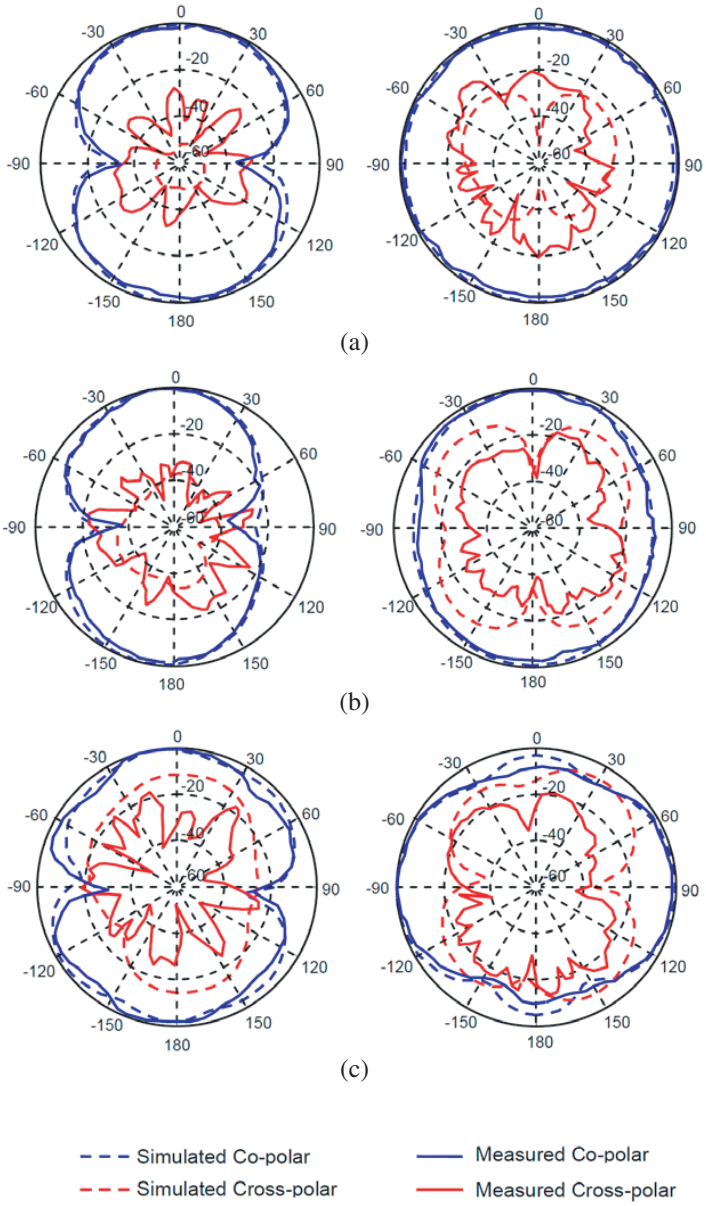

Figure 11. Measured radiation patterns at different frequencies: (a) 4 GHz, (b) 7 GHz, (c) 10 GHz. ($V_{bias} = 2$ V, $f_{notch\ frequency} = 5.1$ GHz).

3. CONCLUSION

A design of UWB planar monopole antenna has been presented and discussed in this paper, which consists of a heart-shaped radiating patch and an elliptical curved ground plane. Experimental results show that the antenna has an impedance bandwidth of 4.25 : 1 for a VSWR less than 2, which covers the entire UWB frequency band. Furthermore, by etching an annular slot loaded with a capacitor in the heart-shaped radiating patch, a band-notched property has been obtained. Finally, by replacing the capacitor with a varactor, a UWB antenna design with a reconfigurable notched band for WLAN services interference rejection has been demonstrated.

The proposed antenna exhibits small size, ultra-wide impedance bandwidth, band-notched reconfigurability, and good radiation performances, which makes it potentially very useful for many UWB applications.

ACKNOWLEDGMENT

This work was supported in part by the Zhejiang Open Foundation of the Most Important Subjects: Information and Communication Engineering under Grant xkxl1504, in part by the National Natural Science Foundation of China (NSFC) under Grant 61501274 and Grant 61571251, and in part by the K. C. Wong Magna Fund in Ningbo University.

REFERENCES

1. Federal Communications Commission, Washington, DC, "FCC report and order on ultra wideband technology," 2002.
2. Liang, J., C. Chiau, X. Chen, and C. Parini, "Study of a printed circular disc monopole antenna for UWB systems," *IEEE Trans. Antennas Propag.*, Vol. 53, No. 11, 3500–3504, Nov. 2005.
3. Xu, H.-Y., H. Zhang, K. Lu, and X.-F. Zeng, "A holly-leaf-shaped monopole antenna with low RCS for UWB application," *Progress In Electromagnetics Research*, Vol. 117, 35–50, 2011.
4. Lu, J. and C. Yeh, "Planar broadband arc-shaped monopole antenna for UWB system," *IEEE Trans. Antennas Propag.*, Vol. 60, No. 7, 3091–3095, May 2012.
5. Dikmen, C. M., S. Cimen, and G. Cakir, "Planar octagonal-shaped UWB antenna with reduced radar cross section," *IEEE Trans. Antennas Propag.*, Vol. 62, No. 6, 2946–2953, Jun. 2014.
6. Alsath, M. and M. Kanagasabai, "Compact UWB monopole antenna for automotive communications," *IEEE Trans. Antennas Propag.*, Vol. 63, No. 9, 4204–4208, May 2015.
7. Bahadori, K. and Y. Rahmat-Samii, "A miniaturized elliptic-card UWB antenna with WLAN band rejection for wireless communications," *IEEE Trans. Antennas Propag.*, Vol. 55, No. 11, 3326–3332, Nov. 2007.
8. Cho, Y., K. Kim, D. Choi, S. Lee, and S. Park, "A miniature UWB planar monopole antenna with 5-GHz band-rejection filter and the time-domain characteristics," *IEEE Trans. Antennas Propag.*, Vol. 54, No. 5, 1453–1460, May 2006.
9. Dissanayake, T. and K. P. Esselle, "Prediction of the notch frequency of slot loaded printed UWB antennas," *IEEE Trans. Antennas Propag.*, Vol. 55, No. 11, 3320–3325, Nov. 2007.
10. Dong, Y. D., W. Hong, Z. Q. Kuai, and J. X. Chen, "Analysis of planar ultrawideband antennas with on ground slot band notched structures," *IEEE Trans. Antennas Propag.*, Vol. 57, No. 7, 1886–1893, 2009.
11. Horestani, A. K., Z. Shaterian, J. Naqui, F. Martín, and C. Fumeaux, "Reconfigurable and tunable s-shaped split-ring resonators and application in band-notched UWB antennas," *IEEE Trans. Antennas Propag.*, Vol. 64, No. 9, 3766–3776, Jun. 2016.
12. Peng, L. and C. Ruan, "UWB band-notched monopole antenna design using electromagnetic-bandgap structures," *IEEE Trans. Antennas Propag.*, Vol. 59, No. 4, 1074–1081, Mar. 2011.
13. Fallahi, R., A. A. Kalteh, and M. G. Roozbahani, "A novel UWB elliptical slot antenna with band-notched characteristics," *Progress In Electromagnetics Research*, Vol. 82, 127–136, 2008.
14. Nikolaou, S., N. D. Kingsley, G. E. Ponchak, J. Papapolymerou, and M. M. Tentzeris, "UWB elliptical monopoles with a reconfigurable band notch using MEMS switches actuated without bias lines," *IEEE Trans. Antennas Propag.*, Vol. 57, No. 8, 2242–2251, 2009.
15. Antonino-Daviu, E., M. Cabedo-Fabres, M. Ferrando-Bataller, and A. Vila-Jamenez, "Active UWB antenna with tunable band-notched behavior," *Electronics Lett.*, Vol. 43, No. 18, 959–960, 2007.
16. Aghdam, S. A., "Reconfigurable UWB antenna using a switchable PIN diode and tunable varactor diode for band rejection behavior," *IEEE Trans. Antennas Propag.*, Vol. 61, No. 10, 5223–5228, Oct. 2013.
17. Hua, C., Y. Lu, and T. Liu, "Printed UWB heart-shaped monopole antenna with band-notch reconfigurability," *IEEE Trans. Antennas Propag.*, Vol. 63, No. 8, 3345–3353, Aug. 2015.
18. Hong, C., C. Ling, I. Tarn, and S. Chung, "Design of a planar ultrawideband antenna with a new band-notch structure," *IEEE Trans. Antennas Propag.*, Vol. 55, No. 12, 3391–3397, 2007.

19. Skyworks Solutions, Inc., 2015, [Online]. Available: http://www. skyworksinc.com/.
20. Nguyen-Trong, N., T. Kaufmann, L. Hall, and C. Fumeaux, "Analysis and design of a reconfigurable antenna based on half-mode substrate-integrated cavity," *IEEE Trans. Antennas Propag.*, Vol. 63, No. 8, 3345–3353, Aug. 2015.
21. Zhang, K., Y. Li, and Y. Long, "Band-notched UWB printed monopole antenna with a novel segmented circular patch," *IEEE Antennas and Wireless Propag. Letters*, Vol. 9, 1209–1212, 2010.
22. Li, T., H. Zhai, C. Zhu, L. Li, C. Liang, and Y. Han, "Design and analysis of compact printed dual band-notched ultrawideband (UWB) antenna," *Journal of Electromagnetic Waves and Applications*, Vol. 27, No. 5, 560–571, 2013.